Table IV. Temperature-Composition Data for the Upper and Lower Surfaces of Heterogeneity

Lower

70 MEK/30 SBA		50 MEK/50 SBA		30 MEK/70 SBA	
% HOH	t, °C	% HOH	t, °C	% HOH	t, °C
22.0	*a*	22.7	*a*	34.8	*a*
31.8	52.2	30.7	*a*	41.6	*a*
40.4	40.6	41.9	58.5	43.8	59.0
55.2	37.0	51.1	51.9	45.2	56.0
65.6	88.8	61.2	50.3	55.9	46.6
75.0	48.6	74.7	57.2	61.9	45.3
80.3	*a*			65.5	44.7
				75.6	47.5
				79.5	55.8

Upper: Constant % HOH = 45.0

% MEK	t, °C
10.1	92
28.8	114
39.3	121
44.3	141

cst[b]	SBA-HOH	113.8 °C (*1*)
cst	MEK-HOH	142.0 °C (*2*)

Tie Lines at 51.5 °C

	MEK	SBA	HOH
(1)			
bottom	14	16	70
top	35	22	43
(2)			
bottom	18	12	70
top	47	33	20

[a] Homogeneous to boiling at 1 atm. [b] Critical solution temperature.

perature now drops until, in theory, the eutectic is reached. In practice, the eutectic is not reached because methyl ethyl ketone refuses to crystallize; a glassy mass is obtained. This investigation was completed previously (*2*).

Similar predictions apply to system *sec*-butyl alcohol–HOH, even to the impossibility of realizing the eutectic, and for the same reason. The $L_1 \rightarrow L_2$ + ice transformation occurs at −5.2 °C. Mixtures of *sec*-butyl alcohol and water were cooled in liquid nitrogen and thermal analysis conducted, using a recording potentiometer.

The data of Table IV, shown in Figure 9, were plotted temperature vs. % HOH for three pseudobinary systems. In each there occurs a minimum in temperature between 50 and 60% HOH. Alternatively when temperature is plotted vs. % MEK for fixed water content a set of curves each with a maximum at 50% MEK results. Hence the lower surface of the heterogeneous volume may be roughly described as saddle-shaped.

The upper surface drops from 114 °C on the SBA–HOH side to a minimum (at constant water content = 45%) around 10% MEK (see Figure 9) and then rises to 142 °C on the MEK–HOH side. Along the 50 MEK/50 SBA–HOH line it falls from 130 °C to below 114 °C. The system • is outside the heterogeneous region at all temperature studied (up to 200 °C).

Also shown in Figure 9 are two tie lines at 52 °C. The remainder of the isotherm was interpolated from the temperature–composition data of Table IV.

Registry No. MEK, 78-93-3; SBA, 78-92-2.

Literature Cited

(1) Rothmund, V. *Z. Phys. Chem.* **1898**, *26*, 433.
(2) Marshall, A. *J. Chem. Soc.* **1908**, *89*, 1350.
(3) Randall, M.; McKenna, F. E. *J. Am. Chem. Soc.* **1951**, *73*, 4859.
(4) Campbell, A. N.; Kartzmark, E. M.; Falconer, W. E. *Can. J. Chem.* **1958**, *36*, 1475.
(5) Alexejeff, M. W. *Bull. Soc. Chim.* **1882**, *38*, 145.
(6) Campbell, A. N.; Kartzmark, E. M. *Can. J. Chem.* **1963**, *41*, 1088.

Received for review June 19, 1985. Accepted November 18, 1985.

Thermal Conductivity Measurement of Heavy Water over a Wide Range of Temperature and Pressure

Roland Tufeu,* Pierre Bury, and Bernard Le Neindre

L.I.M.H.P., C.N.R.S., Université Paris-Nord, 93430 Villetaneuse, France

New measurements of thermal conductivity coefficients of heavy water have been performed in the temperature range from 210 to 510 °C and in the pressure range from 1 to 100 MPa corresponding to a density range from 3 to 700 kg/m³. Most of the measurements were performed in the supercritical region where the typical enhancement of the thermal conductivity is observed. The experimental values are compared with a recommended correlation.

Introduction

Previously, we have used the classical method of coaxial cylinders to determine the thermal conductivity of some polar fluids, in particular light water (*1*) and ammonia (*2*, *3*), in their supercritical ranges. This stationary method allows one to carry out accurate measurements in large temperature and pressure ranges including the critical region if one takes care to ensure that the convection remains small compared to the heat transfer by conduction.

In this paper, we present a new set of measurements of the thermal conductivity coefficients of heavy water in the temperature range from 210 to 510 °C and the pressure range from 1 to 100 MPa. They complete our first measurements obtained in the liquid range (*4*) and vapor phase (*5*).

Several measurements of the thermal conductivity of heavy water have been previously performed and an extensive list of references has been reported by Matsunaga and Nagashima (*6*). However, there were almost no measurements in the supercritical region and correlations of the thermal conductivity surface in this range are made with difficulty.

Experimental Method

The principle of the coaxial cylinder cell was described previously in several reports (*7*–*9*). The temperature rise in the internal cylinder generates a temperature difference between the cylinders. The thermal conductivity λ is calculated by Fourier's law with a number of corrections to take into account the heat losses by solid interfaces (centering pins, electrical

0021-9568/86/1731-0246$01.50/0

Table I. Thermal Conductivity of Heavy Water

T, K	P, MPa	ρ, kg/m^3	λ_e, W/(M K)	$[(\lambda_e - \lambda_n)/\lambda_e]100$	T, K	P, MPa	ρ, kg/m^3	λ_e, W/(M K)	$[(\lambda_e - \lambda_n)/\lambda_e]100$	T, K	P, MPa	ρ, kg/m^3	λ_e, W/(M K)	$[(\lambda_e - \lambda_n)/\lambda_e]100$
484.70	1.01	5.31	0.0379	2.1	654.33	24.88	406.0	0.3643	−8.13	667.41	40.0	595.3	0.3613	−1.15
544.53	1.00	4.58	0.0419	−1.11	654.20	24.98	420.6	0.3630	−7.61	680.31	0.98	3.5	0.0568	−2.33
543.05	5.05	27.9	0.0563	1.11	654.27	26.01	485.0	0.3464	−4.63	680.27	2.53	9.3	0.0577	−2.50
594.26	1.02	4.25	0.0464	−2.73	654.01	27.58	533.9	0.3485	−2.58	680.32	4.94	18.8	0.0593	−3.14
595.49	5.00	23.0	0.0525	−2.18	658.83	30.0	573.2	0.3582	−1.54	680.86	9.95	41.0	0.0658	−2.95
598.28	10.04	56.5	0.0734	−0.11	653.30	35.0	621.0	0.3794	−0.15	681.15	14.98	68.7	0.0773	−2.30
598.10	11.20	68.0	0.0832	−0.10	653.05	40.05	651.4	0.3929	−0.23	681.69	20.00	105.4	0.0972	−1.42
607.01	1.00	4.05	0.0479	−2.68	654.6	0.97	3.6	0.0533	−2.84	682.35	24.95	160.4	0.1338	0.24
607.17	2.52	10.6	0.0492	−2.88	654.46	2.49	9.5	0.0541	−3.47	683.00	27.47	203.5	0.1659	1.83
607.43	4.94	22.0	0.0525	−3.34	654.36	4.97	19.9	0.0565	−3.36	683.35	30.06	270.5	0.2153	2.81
608.69	9.96	52.7	0.0684	−2.34	654.41	9.97	44.3	0.0647	−3.11	683.43	31.5	318.5	0.2474	2.87
609.89	12.50	75.9	0.0868	−1.22	655.28	14.95	76.6	0.0815	−2.00	683.46	32.6	356.0	0.2667	1.89
611.27	13.47	87.0	0.0974	−0.43	656.10	20.0	128.9	0.1189	−0.45	683.55	33.5	383.9	0.2793	1.25
629.88	0.97	3.79	0.0507	−2.23	656.72	22.0	164.6	0.1509	1.49	683.68	35.0	424.5	0.2940	0.12
629.77	2.49	9.97	0.0518	−2.45	658.50	23.0	184.6	0.1692	2.77	683.70	37.6	477.6	0.3112	−0.97
629.73	4.87	20.5	0.0545	−2.52	658.53	23.96	220.3	0.2090	5.07	683.59	40.0	514.1	0.3259	−0.63
630.64	9.90	47.6	0.0655	−2.14	658.52	24.46	248.5	0.2354	3.29	683.59	45.0	563.6	0.3470	−0.32
631.63	14.96	89.0	0.0937	−0.80	658.54	24.77	270.7	0.2588	2.83	683.26	50.0	598.7	0.3638	−0.03
631.15	17.47	128.1	0.1331	1.17	658.36	24.95	290.5	0.2768	1.09	722.74	0.98	3.31	0.0623	−2.20
636.11	20.03	553.7	0.3699	−3.43	658.45	25.15	307.9	0.2948	1.39	722.62	2.55	8.74	0.0631	−2.32
636.04	20.22	560.3	0.3672	−3.69	658.42	25.35	329.0	0.3096	−0.11	722.54	4.93	17.4	0.0645	−2.67
633.36	30.0	671.8	0.4031	−0.80	658.40	25.55	350.3	0.3223	−0.95	722.50	9.95	37.2	0.0690	−3.15
632.40	40.0	715.0	0.4286	−0.30	658.32	25.60	357.9	0.3227	−2.43	722.45	15.01	60.4	0.0763	−3.24
631.49	50.0	745.5	0.4462	−0.66	658.40	25.65	359.7	0.3260	−1.40	722.38	19.96	87.3	0.0874	−2.67
631.40	51.5	749.3	0.4457	−1.32	658.34	25.83	379.3	0.3305	−2.67	722.90	25.0	120.8	0.1038	−1.85
646.58	0.99	3.77	0.0522	−3.18	658.25	26.0	397.3	0.3326	−3.58	723.62	30.0	163.1	0.1276	−0.52
648.37	2.48	9.59	0.0537	−2.86	658.11	28.0	499.8	0.3311	−4.66	723.74	32.1	185.0	0.1408	0.20
648.73	4.87	19.7	0.0567	−1.75	657.45	30.0	547.8	0.3469	−2.20	724.57	35.0	218.5	0.1621	1.45
648.77	10.03	45.4	0.0654	−2.13	656.80	32.5	583.1	0.3583	−1.77	724.63	37.0	245.3	0.1770	0.82
648.91	13.0	64.2	0.0751	−1.34	656.68	35.0	605.8	0.3691	−1.02	725.2	39.9	286.3	0.2017	1.15
649.34	16.94	97.8	0.0970	−0.74	656.38	40.0	639.2	0.3855	−0.50	725.81	42.1	317.5	0.2200	1.39
649.26	20.09	142.6	0.1343	−0.61	656.08	46.9	671.9	0.3999	−1.10	725.68	43.6	340.3	0.2327	1.34
650.78	22.10	194.3	0.1935	1.15	664.11	21.98	146.9	0.1306	0.57	725.54	45.0	361.2	0.2434	1.07
650.43	22.55	222.8	0.2314	−1.99	666.40	24.95	207.0	0.1827	4.08	725.39	46.1	376.5	0.2516	1.10
650.38	22.82	246.7	0.2619	−7.45	666.17	25.78	239.5	0.2125	5.11	725.27	47.6	397.6	0.2621	0.92
650.35	22.96	264.6	0.2878	−11.04	666.14	26.36	268.5	0.2375	5.30	725.37	50.0	426.3	0.2738	0
650.21	23.07	288.3	0.3198	−17.09	666.10	26.76	292.9	0.2574	5.30	774.48	4.96	16.1	0.0724	−0.69
650.27	23.28	329.9	0.3751	−20.80	666.04	27.14	317.8	0.2754	4.99	774.39	10	33.9	0.0763	−0.88
650.25	23.39	357.9	0.4071	−18.41	665.89	27.32	332.4	0.2859	5.01	774.48	15.1	53.7	0.0814	−1.57
650.14	23.43	375.0	0.4189	−16.71	665.77	27.55	350.1	0.2962	4.65	777.86	65.2	397.2	0.2527	0.51
650.30	23.56	393.6	0.4074	−17.46	665.59	28.63	416.0	0.3177	1.88	776.75	75.0	463.4	0.2886	0.65
650.32	23.72	420.0	0.3931	−15.80	665.38	30.10	475.5	0.3259	−0.82	776.44	80.1	491.6	0.3020	0
650.18	24.07	462.4	0.3626	−12.76	665.25	35.05	562.0	0.3472	−1.77	775.87	90.1	537.8	0.3361	2.50
650.19	25.0	510.1	0.3500	−6.43	665.31	0.95	3.50	0.0551	−2.01	775.74	99.8	573.3	0.3579	−2.60
650.30	26.3	543.1	0.3494	−4.31	665.31	2.49	9.35	0.0561	−1.94	778.83	0.97	3.04	0.0696	−2.48
650.47	27.6	563.8	0.3551	−2.80	665.23	4.99	19.5	0.0583	−2.15	778.82	2.57	8.12	0.0699	−3.09
650.42	30.0	594.0	0.3668	−1.27	665.49	9.99	43.0	0.0650	−3.12	778.81	4.93	15.9	0.0711	−3.25
650.43	35.0	633.1	0.3843	−0.39	666.52	14.95	72.7	0.0792	−1.92	779.53	29.96	124.4	0.1079	−2.55
650.65	40.0	659.4	0.3967	−0.36	667.10	20.01	116.5	0.1068	−0.58	780.24	35.0	154.7	0.1224	−1.97
650.84	45.0	680.0	0.4094	0.08	667.10	22.52	150.2	0.1354	3.12	780.13	40.1	190.2	0.1400	−1.57
650.30	50.0	699.1	0.4216	0.33	669.22	25.29	203.4	0.1779	4.27	780.99	45.0	226.9	0.1600	−0.69
650.64	0.98	3.70	0.0529	−2.68	669.13	25.91	223.4	0.1958	5.07	781.58	50.05	267.5	0.1818	−0.32
650.70	2.47	9.51	0.0540	−2.81	669.11	26.34	239.7	0.2084	4.74	781.14	55.1	310.5	0.2053	0
650.89	4.96	19.9	0.0561	−3.43	669.06	26.57	249.7	0.2172	5.02	782.02	60.0	348.2	0.2266	0.57
652.63	9.96	44.5	0.0650	−2.57	668.92	26.76	259.6	0.2249	4.83	781.19	70.1	422.7	0.2656	0.25
653.56	14.96	77.4	0.0826	−1.30	669.08	26.95	267.1	0.2280	3.75	780.56	80.0	481.5	0.2955	−0.36
653.85	19.98	132.0	0.1221	−1.5	669.19	27.36	286.7	0.2442	4.24	782.81	0.95	2.95	0.0706	−1.75
655.24	22.47	183.1	0.1721	2.47	669.09	27.58	300.0	0.2534	3.92	782.34	10.1	33.8	0.0760	−2.60
655.04	23.27	216.2	0.2085	1.78	669.14	27.78	310.4	0.2613	4.15	782.01	20.1	74.0	0.0877	−3.16
654.85	23.79	253.8	0.2536	−0.63	669.09	27.87	316.4	0.2654	4.11	782.44	30.2	124.5	0.1080	−2.78
654.75	24.09	285.9	0.2884	−5.10	669.07	28.00	324.1	0.2702	3.95	783.47	40.2	187.8	0.1385	−1.95
654.66	24.28	313.6	0.3178	−7.75	669.04	28.07	328.5	0.2741	4.29	784.38	50.2	264.2	0.1798	−0.53
654.65	24.38	327.9	0.3336	−7.69	668.88	28.17	336.8	0.2786	3.92	784.59	60.4	345.7	0.2250	0.43
654.55	24.48	345.8	0.3508	−7.63	668.79	28.9	378.6	0.2958	1.91	784.51	70.2	415.5	0.2632	0.8
654.49	24.58	362.4	0.3601	−7.95	668.45	30.0	433.7	0.3083	−1.28	785.49	80.0	470.3	0.2915	0.3
654.47	24.68	377.0	0.3663	−7.50	668.32	32.7	506.6	0.3288	−1.60	784.73	90.0	518.6	0.3196	0.7
654.41	24.78	391.6	0.3668	−7.76	668.04	35.2	547.2	0.3398	−2.12	784.40	95.0	539.1	0.3308	0.52
										785.05	99.1	552.7	0.3400	0.84

wires, and thermocouples) (Q_p), and the heat transferred by convection (Q_c) and radiation (Q_r)

$$\lambda = (K/\Delta T)(Q - Q_p - Q_r - Q_c) \quad (1)$$

In eq 1, K is the constant of the cell, ΔT the temperature difference, and Q the heat generated in the inner cylinder.

To determine the parallel conduction which is a function of the temperature and the thermal conductivity of the sample, a calibration was made with noble gases at 1 MPa for Xe, Kr, and Ar and at 10 MPa for Ne and He. This was done to avoid accommodation effects.

The convection which takes place in the cell is assumed to

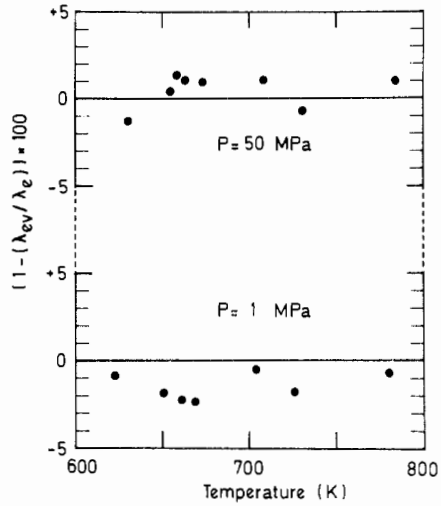

Figure 1. Thermal conductivity of H_2O: comparison between our experimental values λ_e and critically evaluated experimental data λ_{ev} reduced to a uniform grid (*11*).

be laminar. In that case, the correction for convection is approximated by the relation (*10*)

$$Q_c = (\mathrm{Ra}2\pi r/720)\lambda\Delta T \quad (2)$$

where Ra is the Rayleigh number and r the radius of the inner cylinder (r = 0.01 m).

Water was considered a transparent fluid and the classical Stefan–Boltzmann law is used for the correction of radiation

$$Q_r = 4\epsilon\sigma S\Delta T T^3 \quad (3)$$

where ϵ is the emissivity of silver, S the mean emissive area, and σ the Stefan–Boltzmann constant. No noticeable change in the emissivity of silver was observed up to 500 °C.

Apparatus and Experimental Procedure

The cell is made of silver and set up in vertical position for a better uniformity of the radial temperature gradient. The gap between cylinders is 0.2 mm. The cell is sealed, and thus the heavy water is isolated from thermocouples and electrical wires and spurious effects due to the electrical conduction of the sample fluid are avoided. A new method was used to machine and to solder together the different parts of the cell in order to increase its life and performance. To generate the heat inside the inner cylinder, an electric current is passed through a thin platinum wire (0.3 mm diameter) wound on an alumina rod. Pt/Pt–Rh 10% thermocouples are used to measure the temperature difference and the temperature inside the external cylinder. The cell is set up in a high-pressure vessel made of high resistance steel. The pressure vessel is inserted in a thermostat made of copper. The electrical power to the wires wound on the copper furnace is supplied by a power controller. Several thermocouples located at different levels in the furnace control the longitudinal temperature gradients. By means of a long thin silver capillary tubing the cell is connected to a bellows of about 200 cm^3 located in the lower part of the high-pressure vessel at room temperature. The bellows is compressed by nitrogen.

A full description of the apparatus is reported in ref *7–9*.

To determine the thermal conductivity, the various quantities in the relation 1 must be measured. The power Q was obtained from measurements of the heater voltage and current. The current was determined from the measurement of the voltage at terminals of a standard resistor (0.001 Ω). The geometrical constant K of the cell was estimated from a measurement of its electrical capacitance. The temperature difference is measured at four different levels by eight thermocouple wires in series. Their emf is amplified by a Keithley nanovoltmeter amplifier. All these three voltages with the emf corresponding to the temperature measurement are read on a calibrated voltmeter.

The temperature assigned to the measurement of the thermal conductivity was obtained by adding to the temperature measured in the external cylinder half the temperature difference between the cylinders.

The pressure of nitrogen is measured by two Heise Bourdon gauges having different pressure ranges (0–30 and 0–150 MPa).

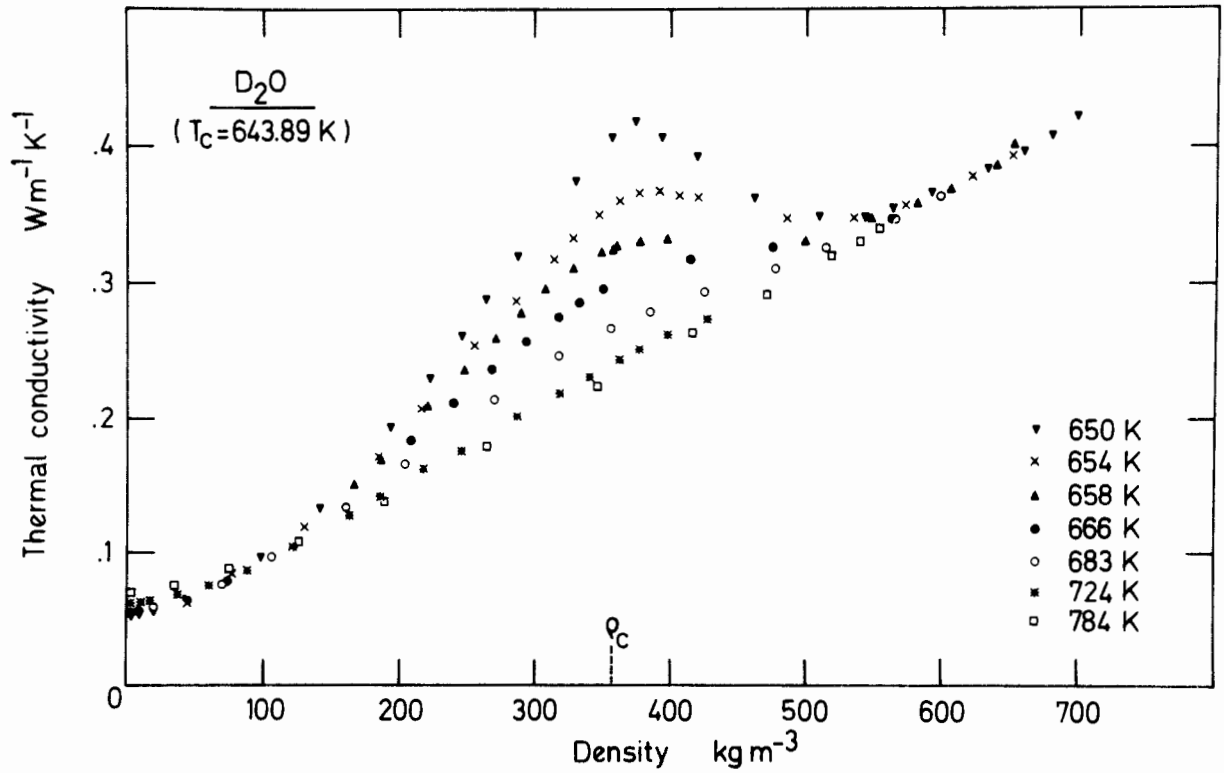

Figure 2. Thermal conductivity of D_2O as a function of density at quasi-constant temperatures.

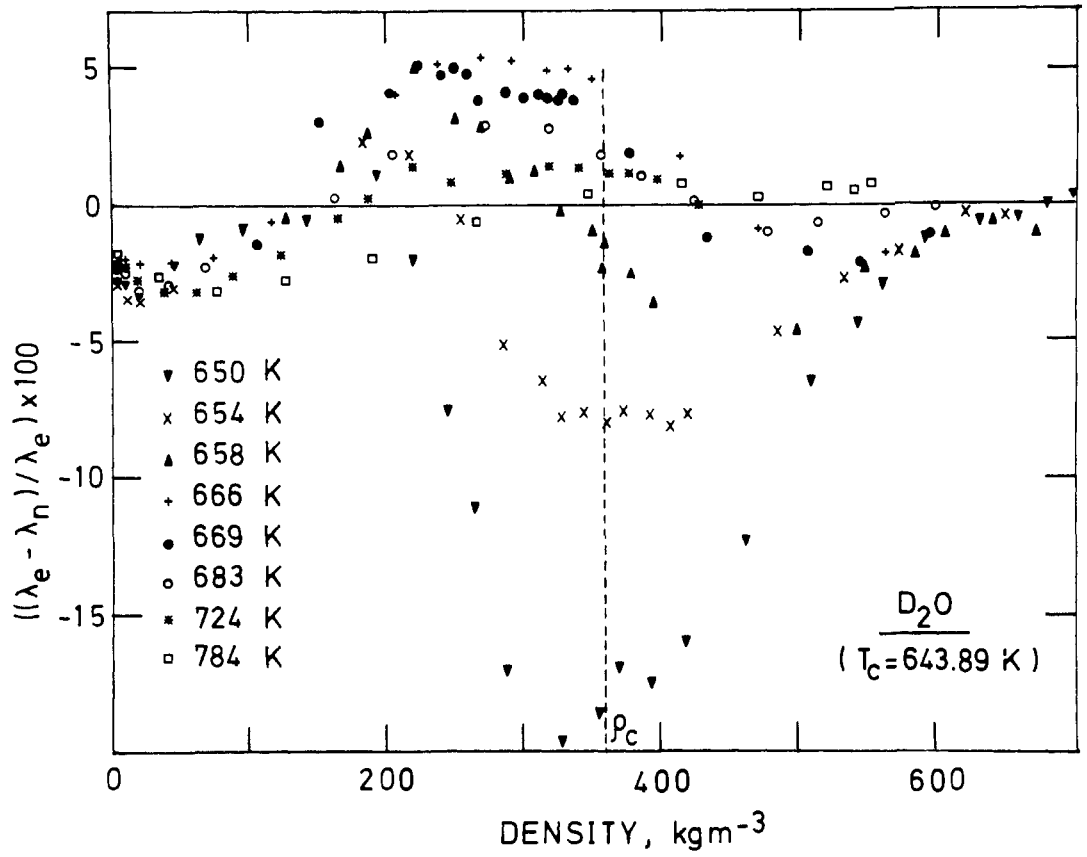

Figure 3. Thermal conductivity of D_2O: comparison between our experimental values λ_e and the values λ_n calculated from eq B1–B11 of ref *6* at temperatures larger than the critical temperature.

The purity of the sample was 99.8% (0.2% light water impurity).

Results

In order to check the 2% estimated accuracy of our D_2O data, the thermal conductivity of H_2O has been measured with the same cell in the same temperature and pressure ranges. As shown in Figure 1, our experimental values obtained for the 1 MPa and 50 MPa isobars and the critically evaluated data reduced to a uniform grid reported in ref. *11* agree well within the assigned tolerances (3% for the 1 MPa isobar and 8% for the 50 MPa isobar).

About 200 experimental points were measured. Most of the measurements were carried out above the critical temperature (T_c = 643.89 K) along quasi-isotherms up to 784 K. The temperature change along a quasi-isotherm is related to the change in the temperature gradient in the sample and in the heat-transfer modification between the cell and the high-pressure vessel.

The density range covered by these experiments extends from 3 to 700 kg m^{-3} as shown in Figure 2. For a consistent comparison with the correlation proposed by Matsunaga and Nagashima (*6*), the densities ρ reported in column 3 of Table I have been calculated from the equation of state reported by Hill et al. (*12*), though a scaled equation of state would be more accurate in the critical range (*13*).

The comparison between our data and the values calculated by using eq 7 of ref *6* is reported in column 5 of Table I and shown in Figure 3.

Large deviations are noted for isotherms close to the critical point (up to 20% at $T - T_c \simeq 6.3$ K and $\rho = \rho_c$). However, it can be seen that good agreement exists outside the critical range. It should be noted that the correlation was made before experimental data existed over much of the critical range and that, consequently, no tolerance is quoted by Matsunaga in the range $0.99 < T/T_c < 1.05$ and $0.8 < \rho/\rho_c < 1.2$.

Conclusion

In this paper we have presented new results on the thermal conductivity of heavy water mainly at temperatures larger than the critical temperature over a wide density range. The present data should be important for making a correlation with greater accuracy in the critical region.

Registry No. D_2O, 7789-20-0.

Literature Cited

(1) Le Neindre, B.; Tufeu, R.; Bury, P.; Sengers, J. V. *Ber. Bunsenges. Phys. Chem.* **1973**, *77*, 262–275.
(2) Tufeu, R.; Letalef, A.; Le Neindre, B. In "Proceedings of the 8th Symposium on Thermophysical Properties"; Sengers, J. V., Ed.; American Society of Mechanical Engineers: New York, 1982; Vol. I, p 451.
(3) Tufeu, R.; Ivanov, D. Y.; Garrabos, Y.; Le Neindre, B. *Ber. Bunsenges. Phys. Chem.* **1984**, *88*, 422–427.
(4) Le Neindre, B.; Bury, P.; Tufeu, R.; Vodar, B. *J. Chem. Eng. Data* **1976**, *21*, 265–274.
(5) Bury, P.; Le Neindre, B.; Tufeu, R.; Johannin, P.; Vodar, B. *Int. Conf. Prop. Steam., [Proc.], 7th, Tokyo, 1968* **1970**, C2.
(6) Matsunaga, N.; Nagashima, A. *J. Phys. Chem. Ref Data* **1983**, *12*, 933–966.
(7) Le Neindre, B. Ph.D. Thesis, Univeristy of Paris, 1969.
(8) Tufeu, R. Ph.D. Thesis, University of Paris, 1971.
(9) Bury, P. Thesis, University of Paris, 1971.
(10) Johannin, P. Ph.D. Thesis, University of Paris, 1958.
(11) Sengers, J. V.; Watson, J. T. R.; Basu, R. S.; Kamgar-Parsi, B.; Hendricks, R. C. *J. Phys. Chem. Ref. Data* **1984**, *13*, 893–933.
(12) Hill, P. G.; Macmillan, R. D. C.; Lee, V. *J. Phys. Chem. Ref. Data* **1982**, *11*, 1–14.
(13) Sengers, J. V.; Levelt-Sengers, J. M. H. *Int. J. of Thermophys.* **1984**, *5*, 195–208.

Received for review May 13, 1985. Revised manuscript received October 15, 1985. Accepted November 11, 1985.